High-temperature signatures of quantum criticality in heavy-fermion systems



2010 J. Phys.: Condens. Matter 22 164203

(http://iopscience.iop.org/0953-8984/22/16/164203)

J. Phys.: Condens. Matter **22** (2010) 164203 (6pp) doi:10.1088/0953-8984/22/16/164203

# High-temperature signatures of quantum criticality in heavy-fermion systems

**J Kroha[1], M Klein[2], A Nuber[2], F Reinert[2,3], O Stockert[4] and H v Löhneysen[5,6]**

[1] Physikalisches Institut and Bethe Center for Theoretical Physics, Universität Bonn, Nussallee 12, 53115 Bonn, Germany
[2] Experimentelle Physik II, Universität Würzburg, Am Hubland, 97074 Würzburg, Germany
[3] Forschungszentrum Karlsruhe, Gemeinschaftslabor für Nanoanalytik, 76021 Karlsruhe, Germany
[4] Max Planck Institute for Chemical Physics of Solids, Nöthnitzer Straße 40, 01187 Dresden, Germany
[5] Physikalisches Institut, Universität Karlsruhe, 76128 Karlsruhe, Germany
[6] Forschungszentrum Karlsruhe, Institut für Festkörperphysik, 76021 Karlsruhe, Germany

E-mail: kroha@physik.uni-bonn.de

Received 25 June 2009, in final form 22 December 2009
Published 30 March 2010
Online at stacks.iop.org/JPhysCM/22/164203

**Abstract**
We propose a new criterion for distinguishing the Hertz–Millis (HM) and the local quantum critical (LQC) mechanism in heavy-fermion systems with a magnetic quantum phase transition (QPT). The criterion is based on our finding that the complete spin screening of Kondo ions can be suppressed by the Ruderman–Kittel–Kasuya–Yosida (RKKY) coupling to the surrounding magnetic ions even without magnetic ordering and that, consequently, the signature of this suppression can be observed in spectroscopic measurements above the magnetic ordering temperature. We apply the criterion to high-resolution photoemission measurements on $CeCu_{6-x}Au_x$ and conclude that the QPT in this system is dominated by the LQC scenario.

(Some figures in this article are in colour only in the electronic version)

## 1. Introduction

At a second-order phase transition the characteristic timescale of the order-parameter fluctuations diverges (critical slowing down), because the energy difference between the ordered and the disordered phases, i.e. the fluctuation energy $\omega_{\rm fl}$, vanishes continuously at the transition. If the phase transition occurs at a finite critical temperature $T_{\rm c}$, quantum fluctuations of the order parameter are always cut off by the temperature $T$, since $T \approx T_{\rm c} > \omega_{\rm fl}$, and the order-parameter fluctuations are thermally excited, i.e. incoherent (dark shaded regions in figures 1(a) and (b)). In this sense, such a phase transition is classical. If, however, the transition is tuned to absolute zero temperature by a non-thermal control parameter, the system is at the critical point in a quantum coherent superposition of the degenerate ordered and disordered states. The transition is called a quantum phase transition (QPT), for reviews see [1, 2]. The excitation spectrum above this quantum critical state may be distinctly different from the excitations of either phase, the disordered and the ordered one. Therefore, the physical properties are not only dominated by the quantum fluctuations between these phases at $T = 0$, but show also unusual temperature dependence essentially due to thermal excitation of the anomalous spectrum, so that the quantum critical behavior extends up to elevated temperatures (regions marked 'QCF' in figures 1(a) and (b)).

In particular, in a number of heavy-fermion (HF) compounds, where heavy quasiparticles are formed due to the Kondo effect and subsequent lattice coherence, a magnetic phase transition may be suppressed to $T = 0$ by chemical composition, pressure or magnetic field. Two types of scenarios are, in principle, conceivable in these metallic systems.

In the first scenario, the quasiparticle system undergoes a spin-density wave (SDW) instability at the quantum critical point (QCP), as described by the theory of Hertz [3] and Millis [4] (HM scenario). The instability can be caused by various types of residual spin exchange interactions. In this

 

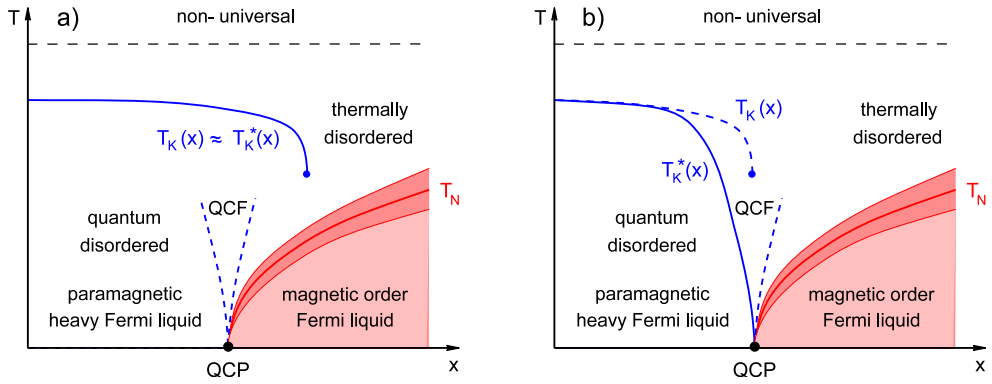


**Figure 1.** Generic phase diagrams of a magnetic QPT in an HF system, driven by an antiferromagnetic RKKY coupling (parametrized by a non-thermal control parameter $x$) for (a) the HM and (b) the LQC scenario. For both scenarios the predicted behavior of the spin screening scale on the lattice, $T_K^\star$, *including* the presence of quantum critical fluctuations (QCF), and as extracted from local Kondo-ion spectra *without* lattice coherence or QCF, $T_K$, is also shown (see the text for details). The maximum antiferromagnetic RKKY coupling, $x_m$, where single-ion Kondo screening terminates, is marked by a black dot.

scenario the Landau Fermi-liquid, albeit undergoing magnetic ordering, prevails, and the Kondo temperature $T_K$ remains finite across the QPT.

In the second type of scenario, the Kondo effect and, hence, the very formation of heavy fermionic quasiparticles is suppressed. This may occur due to magnetic coupling to the surrounding moments [5, 6] or possibly due to fluctuations of the Fermi volume involved with the onset of Kondo screening in an Anderson lattice system [7]. Both the bosonic order-parameter fluctuations and the local fermionic excitations then become critical at the QPT [5, 6]. In this case the system is in a more exotic, genuine many-body state which is not described by the Landau Fermi-liquid paradigm. For the critical breakdown of Kondo screening due to magnetic fluctuations the term 'local quantum critical (LQC)' has been coined [5].

Unambiguously identifying the quantum critical scenario from the low-$T$ behavior, not to mention predicting the scenario for a given system, has remained difficult. One reason for this is that the precise critical behavior is not known because of approximate assumptions implicit in the theoretical description of either one scenario, HM or LQC. While the HM theory [3, 4] pre-assumes the existence of fermionic quasiparticles with only bosonic, critical order-parameter fluctuations, the extended dynamical mean field theory (EDMFT) description of the LQC scenario [5, 6] neglects possible changes of the critical behavior due to spatially extended critical fluctuations. Motivated by our recent ultraviolet photoemission spectroscopy (UPS) [8] and x-ray photoemission spectroscopy (XPS) [10] measurements of the Kondo resonance at elevated $T$ across the Au-concentration range of the QPT in $CeCu_{6-x}Au_x$, we here put forward a criterion to predict the quantum critical scenario of an HF system from its high-$T$ behavior around and above the single-ion Kondo temperature $T_K$. As seen below, this criterion is derived from the fact that the complete Kondo screening breaks down when the dimensionless RKKY coupling $y$ between Kondo ions exceeds a certain strength $y_m$, even when critical fluctuations due to magnetic ordering do not play a role. $y_m$ can be expressed in a universal way in terms of the bare single-ion Kondo temperature $T_K(0)$ only, see equation (5) below. This breakdown is related to the unstable fixed point of the two-impurity Kondo model which separates the Kondo-screened and the inter-impurity (molecular) singlet ground states of this model [11]. In the present paper we explore and utilize its signatures at temperatures well above the lattice coherence temperature $T_{coh}$ and the magnetic ordering or Néel temperature $T_N$, i.e. in a region where neither critical fluctuations of the Fermi surface [7] nor the magnetic order parameter play a role.

In the following section 2 we present our calculations of the high-temperature signatures of the RKKY-induced Kondo breakdown using perturbative renormalization group as well as self-consistent diagrammatic methods. In section 3 we briefly recollect the UPS results for $CeCu_{6-x}Au_x$ [8] and interpret them in terms of the high-$T$ signatures of Kondo breakdown. Some general conclusions are drawn in section 4.

## 2. Theory for single-ion Kondo screening in a Kondo lattice

We consider an HF system described by the Kondo lattice model of local 4f spins $S = 1/2$ with the exchange coupling $J$ to the conduction electrons and the density of states at the Fermi level, $N(0)$, for temperatures well above $T_{coh}$, $T_N$. In this regime controlled calculations of renormalized perturbation theory in terms of the single-impurity Kondo model are possible and can be directly compared to experiments [8]. In particular, the RKKY interaction of a given Kondo spin at site 0 with identical spins at the surrounding sites $i$ can be treated as a perturbative correction to the local coupling $J$. We define the single-ion Kondo screening scale $T_K(x)$ as the energy scale below which a single 4f spin forms a singlet with the conduction electron system. Because of the RKKY-induced corrections to $J$, this scale will depend on the ratio $k_F a$ of the lattice constant $a$ and the Fermi wavelength $\lambda_F = 2\pi/k_F$ and, hence, on the concentration of doping atoms, e.g. on the

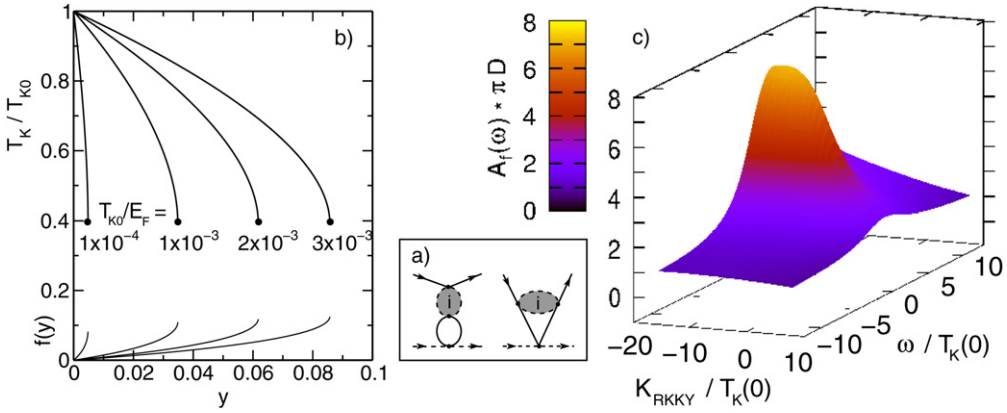


**Figure 2.** (a) Leading-order RKKY-induced corrections to the local spin exchange coupling. Solid and dashed lines represent conduction electron and impurity spin (pseudofermion) propagators, respectively. (b) The single-impurity Kondo scale $T_K(y)$ with RKKY corrections to the local exchange coupling (a) is shown as a function of $y$ for various values of the bare Kondo temperature $T_K(0)$. The effective perturbation parameter $f(y)$ is also shown. (c) NCA result for the f spectral density on a single Kondo ion, including RKKY corrections (a) for $T = 2\,T_K(0)$. The steep collapse of the Kondo resonance for increasing antiferromagnetic RKKY coupling $K_{RKKY}$ is clearly seen.

Au content $x$ in $CeCu_{6-x}Au_x$. We emphasize that the single-ion Kondo scale $T_K(x)$ explicitly excludes effects of lattice coherence and of magnetic ordering. These effects modify the screening scale to the lattice Kondo temperature $T_K^\star(x)$ [9]. $T_K(x)$ and $T_K^\star(x)$ are sketched in figure 1. Nevertheless, the single-ion scale $T_K(x)$ has physical relevance, since it is the scale extracted from spectroscopic measurements [8, 10] performed at temperatures $T$ far above the coherence and the magnetic ordering temperatures, $T_{coh}$, $T_N$.

The leading-order direct and exchange corrections to the local spin exchange coupling, $\delta J^{(d)}$, $\delta J^{(ex)}$, are depicted diagrammatically in figure 2(a). As seen from the figure, these corrections involve the full dynamical impurity spin susceptibility (shaded bubbles) on the neighboring impurity sites $i$, $\chi_{4f}(T,0) = (g_L\mu_B)^2 N(0) D_0/(4\sqrt{T_K^2+T^2})$, with the bare band width $D_0 \approx E_F$, the Landé factor $g_L$ and the Bohr magneton $\mu_B$ [12]. Summing over all lattice sites $i \neq 0$ one obtains [8],

$$\delta J^{(d)} = -y\frac{1}{4} J g_i^2 \frac{D_0}{\sqrt{T_K^2+T^2}} \frac{1}{1+(D/T_K)^2} \qquad (1)$$

$$\delta J^{(ex)} = -y\frac{1}{4} J g_i^2 \left(\frac{3}{4} + \frac{T}{\sqrt{T_K^2+T^2}}\right). \qquad (2)$$

Here $g_i = N(0)J_i$ is the dimensionless bare coupling on site $i \neq 0$, $y$ is a dimensionless factor that describes the relation between the RKKY coupling strength and the Au content $x$. In the vicinity of the QPT we assume a linear dependence, $y = \alpha(x + x_0)$, with adjustable parameters $\alpha$ and $x_0$. For simplicity we have chosen $x_0 = 0$ in the following, although in the real compound the RKKY coupling $y$ certainly does not vanish for $x = 0$. This is, however, merely a matter of calibration and not relevant near the QCP. We do not consider a doping dependence of the bare bandwidth $D_0$ or of $N(0)$, since this dependence is smooth and not renormalized by the perturbative renormalization group. In $\delta J^{(d)}$ (first diagram in figure 2(a)) the local spin response $\chi_{4f}(T,\Omega)$ restricts the energy exchange between conduction electrons and local spin, i.e. the (running) band cutoff $D$, to $T_K$. This is described by the last factor in equation (1) (soft cutoff). In $\delta J^{(ex)}$ (second diagram in figure 2(a)) $\chi_{4f}(T,\Omega)$ restricts the conduction electron response to a shell of width $T_K$ around the Fermi energy $E_F$, and suppresses $\delta J^{(ex)}$ compared to $\delta J^{(d)}$ by an overall factor of $\sqrt{T_K^2+T^2}/D_0$, as seen in equation (2). The spin screening scale of this effective single-impurity problem, including RKKY corrections, can now be obtained as the energy scale where the perturbative renormalization group (RG) for the RKKY-corrected spin coupling (taken at $T = 0$) diverges. The one-loop RG equation reads

$$\frac{\mathrm{d}J}{\mathrm{d}\ln D} = -2N(0)[J + \delta J^{(d)}(D) + \delta J^{(ex)}(D)]^2. \qquad (3)$$

Note that in this RG equation the bare bandwidth $D_0$ and the couplings $g_i$ on sites $i \neq 0$ are not renormalized, since this is already included in the full susceptibility $\chi_{4f}$. The essential feature is that for $T = 0$ the direct RKKY correction $\delta J^{(d)}$, equation (1), is inversely proportional to the renormalized Kondo scale $T_K(y)$ itself via $\chi_{4f}(0,0)$. The solution of equation (3) leads to a highly nonlinear self-consistency equation for $T_K(y)$,

$$\frac{T_K(y)}{T_K(0)} = \exp\left\{-\left(\frac{1}{2g} + \ln 2\right)\frac{f(u)}{1-f(u)}\right\}, \qquad (4)$$

with $g = N(0)J$, $f(u) = u - u^2/2$, $u = yg^2 D_0/[4T_K(y)]$. The single-ion Kondo scale without RKKY coupling is $T_K(0) = D_0 \exp[-1/2g]$. Figure 2(b) shows solutions of equation (4) for various values of $T_K(0)$, together with the corresponding values of the effective perturbation parameter $f(y)$. It is seen that this RG treatment is perturbatively controlled in the sense that $f(y) \lesssim 0.1$, i.e. the exponent in equation (4) remains small for all solutions. Remarkably, a solution of equation (4) exists only up to a certain RKKY coupling strength $y_m$. For each value of the bare single-ion

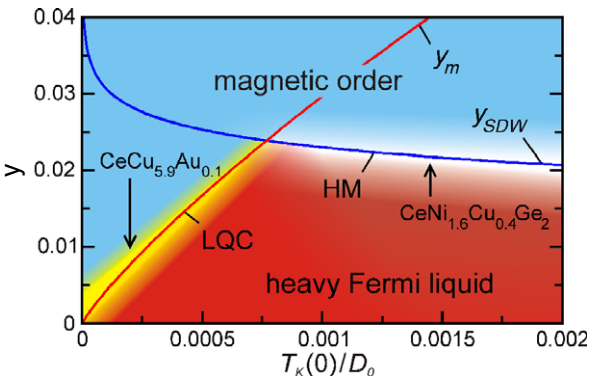


**Figure 3.** Schematic phase diagram of an HF system with a magnetic QPT in the $T_K(0)$–$y$ plane. The line denoted by $y_m$ represents equation (5). At this line $T_K(y)$ undergoes an abrupt step, see the text. The curve denoted by $y_{SDW}$ marks, as an example, an SDW instability of the system. The magnetic phase transition, LQC- or HM-like, occurs at whichever of the two lines is lower for a given system. The arrows indicate estimates [24] for $T_K(0)/D_0$ for $CeCu_{6-x}Au_x$ and $CeNi_{2-x}Cu_xGe_2$.

Kondo temperature, $\tau_K = T_K(0)/D_0$, $y_m$ can be calculated as the point where the derivative $dT_K(y)/dy$ diverges [8],

$$y_m = 3.128\tau_K(\ln\tau_K)^2\left[2 - \ln\frac{\tau_K}{2} - \sqrt{\left(2 - \ln\frac{\tau_K}{2}\right)^2 - 4}\right]. \quad (5)$$

By rescaling $y$ and $T_K(y)$ as $y/y_m$ and $T_K(y)/T_K(0)$, respectively, all $T_K(y)$ curves collapse onto a single, universal curve, shown in the inset of figure 5 below. For $y > y_m$ the RG equation (3) does not diverge, i.e. the Kondo screening breaks down at this maximum RKKY coupling strength $y_m$, even if magnetic ordering does not occur. Therefore, the physical origin of the high-$T$ criterion (5) is different from the well-known Doniach criterion [13] (which reads $T_K(0) \approx y_m N(0) J^2$), even though it yields numerically similar values for $y_m$. According to figure 2(b) a sharp drop of $T_K$ is predicted at $y = y_m$. As seen in figure 2(c), this breakdown of Kondo screening is signaled by a collapse of the Kondo resonance in the local 4f spectrum $A_f(\omega)$ of a single Kondo ion, as the antiferromagnetic RKKY coupling to neighboring Kondo ions is increased. Figure 2(c) shows $A_f(\omega)$ as calculated for the two-impurity Anderson model within the non-crossing approximation (NCA) at $T = 2\,T_K(0)$ [14]. For an efficient implementation of the NCA see [15]. Details of these calculations as well as numerical renormalization group (NRG) studies of this problem will be published elsewhere. The described signatures should be directly observable in spectroscopic experiments at temperatures well above $T_N$, see section 3. We emphasize again that the Kondo breakdown occurs in any case, whether or not magnetic ordering sets in at low $T$.

Therefore, the model predicts two quantum critical scenarios with distinctly different high-$T$ signatures: (1) the heavy Fermi-liquid has a magnetic, e.g. SDW, instability at $T = 0$ for an RKKY parameter $y = y_{SDW} < y_m$, i.e. without breakdown of Kondo screening. In this case, $T_K(y)$, as extracted from high-$T$ UPS spectra, is essentially constant across the QCP but does have a sharp drop at $y = y_m$ inside the region where magnetic ordering occurs at low $T$, see figure 1(a). This corresponds to the HM scenario. (2) Magnetic ordering does not occur for $y < y_m$. In this case the Kondo breakdown at $y = y_m$ implies that the residual local moments order at sufficiently low $T$, i.e. the magnetic QCP coincides with $y = y_m$. Quantum critical fluctuations (not considered in the present high-$T$ theory) will suppress the actual Kondo screening scale $T_K$ below the high-$T$ estimate $T_K$, as shown in figure 1(b). This is the LQC scenario. These predictions are summarized in figure 3 as a phase diagram in terms of the bare Kondo scale $T_K(0)$ and the dimensionless RKKY coupling $y$ [8].

## 3. High-resolution photoemission spectroscopy at elevated temperature

The theory described in the previous section should be applicable quite generally to HF systems with a magnetic QPT.

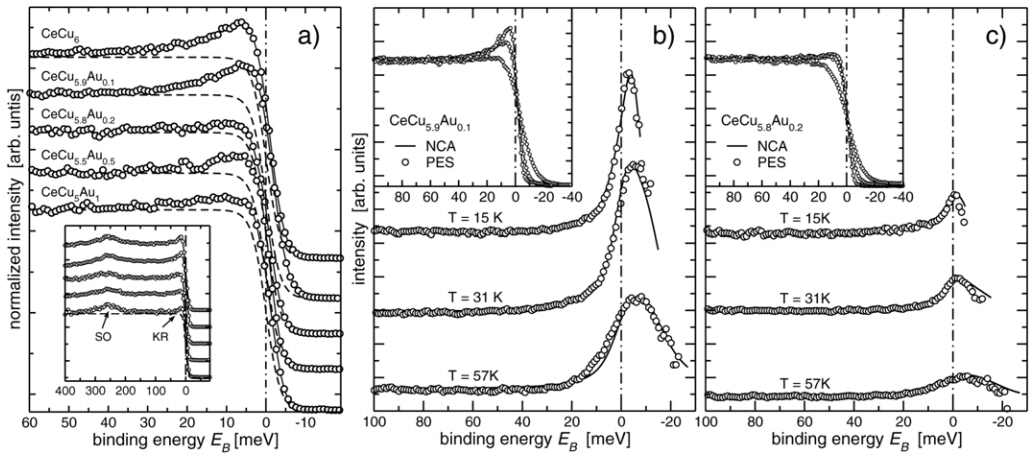


**Figure 4.** (a) Near-$E_F$ spectra of $CeCu_{6-x}Au_x$ for five different Au concentrations at $T = 15$ K. The dashed lines indicate the resolution-broadened FDD at $T = 15$ K. The inset shows a larger energy range including the spin–orbit (SO) satellite at $E_B \approx 260$ meV. See [8] for details of the experimental parameters. (b) and (c) Spectra for $x = 0.1$ and $x = 0.2$, respectively, divided by the FDD, at various $T$. The solid lines are single-impurity NCA fits. The insets in (b) and (c) show the corresponding raw data.

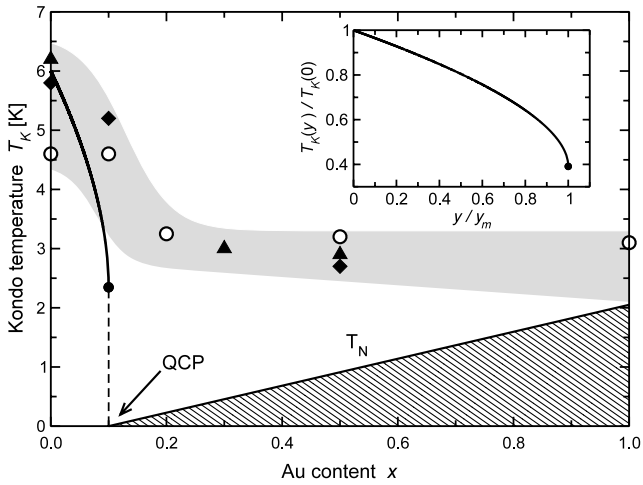


**Figure 5.** Dependence of the Kondo temperature $T_K$ on the Au content $x$, as determined by UPS (open circles), specific heat [28] (triangles), and neutron scattering [21, 29] (diamonds). The error bars are approximately given by the width of the shaded area. The Néel temperature is labeled by $T_N$. The inset and the solid line in the main panel show the universal curve $T_K(y)/T_K(0)$ versus $y/y_m$ as given by equation (4).

Here we apply it to $CeCu_{6-x}Au_x$, which is one of the best characterized HF compounds [16–22, 30]. The Au content $x$ is used to tune the RKKY interaction through the QPT at $x = x_c = 0.1$, and our recent UPS measurements [8] on this compound at elevated $T$ have actually motivated the theoretical study. Details of the sample preparation and measurement procedures can be found in [23, 24]. The UPS measurements were done at $T = 57$, 31, and 15 K, i.e. well above $T_K(0) \approx 5$ K, $T_{coh}$, and above the temperature up to which quantum critical fluctuations extend in $CeCu_{6-x}Au_x$ [29]. Thus they record predominantly the local Ce 4f spectral density which is characterized by an effective *single-ion* Kondo scale $T_K$. This corresponds to the situation for which the calculations in section 2 were done. In figure 4(a) raw UPS Ce 4f spectra are displayed, showing the onset of the Kondo resonance. A sudden decrease of the Kondo spectral weight at or near the quantum critical concentration $x_c$ can already be observed in these raw spectra. The states at energies of up to $5k_BT$ above the Fermi level are accessible by a well established procedure [23, 24] which involves dividing the raw UPS spectra by the Fermi–Dirac distribution function (FDD). The Kondo resonance, which in $CeCu_{6-x}Au_x$ is located slightly above the Fermi level, then becomes clearly visible, see figures 4(b) and (c). These figures clearly exhibit the collapse of the Kondo spectral weight above as compared to below $x_c$. It is in qualitative accordance with the Kondo resonance collapse in the theoretical spectra for $T > T_K(0)$, figure 2(c). To pinpoint the position of the Kondo breakdown more precisely, the single-ion Kondo temperature $T_K$ was extracted from the experimental spectra for various $x$. To that end, we followed the procedure successfully applied to various Ce compounds in the past [25–27, 23, 24]: using the non-crossing approximation (NCA) [15] the Ce 4f spectral function of the single-impurity Anderson model was calculated, including all crystal field and spin–orbit excitations. For each composition $x$ the NCA spectra are broadened by the experimental resolution and fitted to the experimental data, using a single parameter set for all experimental $T$. Using this parameter set, the NCA spectra were then calculated at low temperature, $T \approx 0.1\,T_K$, where $T_K$ was extracted from the Kondo-peak half-width at half-maximum (HWHM) of the NCA spectra. The results are shown in figure 5. The finite Kondo scale extracted from the data for $x > x_c = 0.1$ results from the high-$T$ onset of the Kondo resonance seen in figure 4(c) which, according to our analysis, is expected not to persist to low $T$. Despite an uncertainty in $T_K$, estimated by the width of the shaded area in figure 5, a sudden decrease of $T_K$ is clearly visible. The fact that the sharp $T_K$ drop of the experimental data occurs at (or very close to) the quantum critical concentration $x_c$ suggests that we could identify this drop with the theoretically expected signature of the Kondo breakdown at $y_m$, as illustrated in figure 5. This supports the fact that the QPT in $CeCu_{6-x}Au_x$ follows the LQC scenario driven by intersite magnetic fluctuations, as explained in section 2, and as was previously inferred from inelastic neutron scattering experiments [29]. However, the nearby orthorhombic–monoclinic structural transition occurring at 220 K for $x = 0$ and at 70 K for $x = 0.1$ [30] might also have an effect on the behavior of $T_K$. Therefore, future work has to substantiate the above LQC conjecture, even though across the structural transition the lattice unit cell volume and, hence, the density of states at the Fermi level tend to *increase* smoothly with increasing $x$, leading to an increase rather than a drop of $T_K$.

## 4. Conclusion

Our theoretical analysis predicts generally that an abrupt step of the Kondo screening scale extracted from high-$T$ spectral data should occur in any HF compound with competing Kondo and RKKY interactions, as long as the single-ion Kondo screening scale is larger than the magnetic ordering temperature. Whether this distinct feature is located at the quantum critical control parameter value $x_c$ or inside the magnetically ordered region constitutes a general high-$T$ criterion to distinguish the LQC and HM scenarios. Moreover, this criterion allows us to predict whether a given system should follow the HM or the LQC scenario, once estimates for the bare single-ion Kondo scale $T_K(0)$ and for dimensionless critical coupling strength $y_{SDW}$ for an SDW instability in that system are known. This is indicated in figure 3 for the examples of $CeCu_{6-x}Au_x$ and $CeNi_{2-x}Cu_xGe_2$. A systematical analysis of other HF compounds in this respect is in progress.

## Acknowledgments

We would like to thank F Assaad, L Borda, S Kirchner, A Rosch, and M Vojta for fruitful discussions. This work was supported by DFG through Re 1469/4-3/4 (MK, AN, FR), SFB 608 (JK) and FOR 960 (HvL).

## References


[1] Löhneysen H v, Rosch A, Vojta M and Wölfle P 2007 *Rev. Mod. Phys.* **79** 1015
[2] Gegenwart P, Si Q and Steglich F 2008 *Nat. Phys.* **4** 186
[3] Hertz J A 1976 *Phys. Rev.* B **14** 1165
[4] Millis A 1993 *Phys. Rev.* B **48** 7183
[5] Si Q, Rabello S, Ingersent K and Smith J L 2001 *Nature* **413** 804
[6] Coleman P, Pépin C, Si Q and Ramazashvili R 2001 *J. Phys.: Condens. Matter* **13** R723
[7] Senthil T, Vojta M and Sachdev S 2004 *Phys. Rev.* B **69** 035111
[8] Klein M, Nuber A, Reinert F, Kroha J, Stockert O and Löhneysen H v 2008 *Phys. Rev. Lett.* **101** 266404
[9] Pruschke Th, Bulla R and Jarrell M 2000 *Phys. Rev.* B **61** 12799
[10] Klein M, Kroha J, Löhneysen H v, Stockert O and Reinert F 2009 *Phys. Rev.* B **79** 07511
[11] Jones B A and Varma C M 1987 *Phys. Rev. Lett.* **58** 843
[12] Andrei N, Furuya K and Löwenstein J H 1983 *Rev. Mod. Phys.* **55** 331
[13] Doniach S 1977 *Physica* B&C **91** 231
[14] Keiter H and Kimball J C 1971 *Int. J. Magn.* **1** 233
Grewe N and Keiter H 1981 *Phys. Rev.* B **24** 4420
Grewe N 1993 *Z. Phys.* B **52** 193
Kuramoto Y 1983 *Z. Phys.* B **53** 37
[15] Costi T A, Kroha J and Wölfle P 1996 *Phys. Rev.* B **53** 1850
[16] Löhneysen H v, Pietrus T, Portisch G, Schlager H G, Schröder A, Sieck M and Trappmann T 1994 *Phys. Rev. Lett.* **72** 3262
[17] Löhneysen H v 1996 *J. Phys.: Condens. Matter* **8** 9689
[18] Löhneysen H v, Mock S, Neubert A, Pietrus T, Rosch A, Schröder A, Stockert O and Tutsch U 1998 *J. Magn. Magn. Mater.* **177–181** 12
[19] Stockert O, Löhneysen H v, Rosch A, Pyka N and Loewenhaupt M 1998 *Phys. Rev. Lett.* **80** 5627
[20] Löhneysen H v, Neubert A, Pietrus T, Schröder A, Stockert O, Tutsch U, Löwenhaupt M, Rosch A and Wölfle P 1994 *Eur. Phys. J.* B **5** 447
[21] Stroka B, Schröder A, Trappmann T, Löhneysen H v, Loewenhaupt M and Severing A 1993 *Z. Phys.* B **90** 155
[22] Stockert O, Enderle M and Löhneysen H v 2007 *Phys. Rev. Lett.* **99** 237203
[23] Reinert F, Ehm D, Schmidt S, Nicolay G, Hüfner S and Kroha J 2001 *Phys. Rev. Lett.* **87** 106401
[24] Ehm D, Hüfner S, Reinert F, Kroha J, Wölfle P, Stockert O, Geibel C and Löhneysen H v 2007 *Phys. Rev.* B **76** 045117
[25] Patthey F, Imer J-M, Schneider W-D, Beck H, Baer Y and Delley B 1990 *Phys. Rev.* B **42** 8864
[26] Garnier M, Breuer K, Purdie D, Hengsberger M and Baer Y 1997 *Phys. Rev. Lett.* **78** 4172
[27] Allen J *et al* 2000 *J. Appl. Phys.* **87** 6088
[28] Schlager H G, Schröder A, Welsch M and Löhneysen H v 1992 *J. Low Temp. Phys.* **90** 181
[29] Schröder A, Aeppli G, Coldea R, Adams M, Stockert O, Löhneysen H v, Bucher E, Ramazashvili R and Coleman P 2000 *Nature* **407** 351
[30] Grube K, Fietz W H, Tutsch U, Stockert O and Löhneysen H v 1999 *Phys. Rev.* B **60** 11947